Growth of $In_xGa_{1-x}As$ quantum dots by metal–organic chemical vapor deposition on Si substrates and in GaAs-based lasers

Zaman Iqbal Kazi[a)]
Department of Electrical and Computer Engineering, Nagoya Institute of Technology, Gokiso-cho, Showa-ku, Nagoya 466-8555, Japan

Takashi Egawa and Masayoshi Umeno[b)]
Research Center for Micro-Structure Devices, Nagoya Institute of Technology, Gokiso-cho, Showa-ku, Nagoya 466-8555, Japan

Takashi Jimbo[c)]
Department of Environmental Technology and Urban Planning Graduate School of Engineering, Nagoya Institute of Technology, Gokiso-cho, Showa-ku, Nagoya 466-8555, Japan

(Received 4 December 2000; accepted for publication 3 April 2001)

The growth conditions of low-dimensional dot structures of strained $In_xGa_{1-x}As$ on Si substrates using the Stranski–Krastanov growth mode by metal–organic chemical vapor deposition are optimized. Atomic force microscopy measurement has been performed to characterize the dot structures. The dot density and their size are found to be strongly dependent on the substrate temperature, In content, and V/III ratio. The optimized growth condition was further used to fabricate quantum dot-like laser diodes on Si. The characteristics of the laser diode with an $In_xGa_{1-x}As$ quantum dot-like active region are analyzed. © *2001 American Institute of Physics.* [DOI: 10.1063/1.1375010]

I. INTRODUCTION

The successful growth of reliable GaAs-based heteroepitaxial injection lasers, photodetectors, waveguides, and modulators directly on Si makes the integration of Si electronics with high-speed, low-power optoelectronic functions possible and permits the fabrication of large-scale optoelectronic integrated circuits (OEICs).[1–6] However, ~4% lattice mismatch and ~250% difference in the thermal expansion coefficients between GaAs and Si result in high dislocation densities ($\sim 10^6/cm^2$) at heterointerface.[7] The high magnitude of such dislocation density forms the dark line defect (DLD) networks in epitaxially grown devices.[8–10] As a result, GaAs-based devices, such as lasers on Si degrade rapidly within a few minutes.[11] Though several techniques, such as (1) low temperature growth,[12,13] (2) growth of a strained layer superlattice (SLS) buffer layer such as InGaAs on GaAs/Si,[14] and (3) use of an orientation tilted Si substrate[14,15] have been employed previously, there still remain difficulties with dislocations in GaAs-based devices on Si.

Growth of self-organized quantum dots (QDs) in laser structure emerges as a new approach to enhance the lasing efficiency and reliability of laser diodes.[16,17] Egawa *et al.* have demonstrated AlGaAs/GaAs laser diodes on Si grown by ''droplet'' epitaxy with GaAs island-like active regions.[11] Later, Linder *et al.* reported the growth of a self-organized $In_{0.4}G_{0.6}As$ quantum dot laser on Si substrates by molecular beam epitaxy.[18] However, so far, no QD laser structure has been reported on Si substrate with room temperature (RT) continuous wave operation. The reason is supposed to be due to the nonuniform growth behavior of the dot size and lower density,[19] which fails to enhance the quantum mechanical effect of the lasing action.[20] In this article, the details of the growth mechanism of QD using the Stransky–Krastanov (SK) growth mode, as well as fabrication of lasers on Si, are described.

II. EXPERIMENTAL DETAILS

The dot structures were grown on the (100) n^+-Si substrates oriented 2° off towards the [011] direction using a rf-heated horizontal metal–organic chemical vapor deposition (MOCVD) reactor at atmospheric pressure. Trimethylgallium (TMG) and trimethylaluminum (TMA) were chosen as group-III sources and arsine (AsH_3) was chosen as the group-V source. Hydrogen selenide (H_2Se) and diethylzinc (DEZ) were injected as the *n* and *p* dopants, respectively. Hydrogen was used as the carrier gas. After loading the Si substrate in the MOCVD reactor chamber, it was heated in H_2 atmosphere at 1000 °C for 10 min in order to remove the native oxide from the substrate surface. Then, a 1 μm thick GaAs buffer layer was grown at 650 °C. During the growth of the n^+-GaAs buffer layer, the substrate temperature was cycled five times from 350 to 850 °C in an AsH_3 atmosphere in order to reduce the threading dislocation in the GaAs layer.[21] The growth of dots was carried out on the GaAs buffer layer by considering different parameters, such as total H_2 flow rate, growth temperature, AsH_3 flow rate, V/III ratio,

[a)]Present address: Fujitsu Quantum Devices Ltd., 1000 Kamisukiawara, Showa-chou Nkakakoma-gun, Yamanashi-ken 409-3883, Japan.
[b)]Present address: Department of Electronic Engineering, Faculty of Engineering, Chubu University, 1200 Matsumoto Kasugai 487-8501 Japan.
[c)]Author to whom correspondence should be addressed; electronic mail: jimbo@elcom.nitech.ac.jp

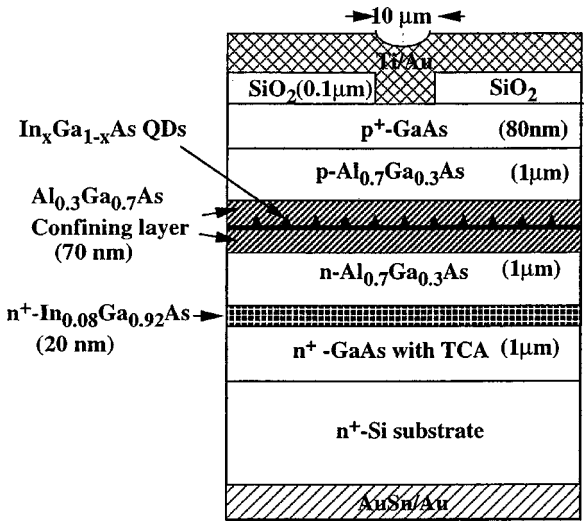

FIG. 1. Schematic structure of the $In_xGa_{1-x}As$ quantum dot-like laser on a Si substrate.

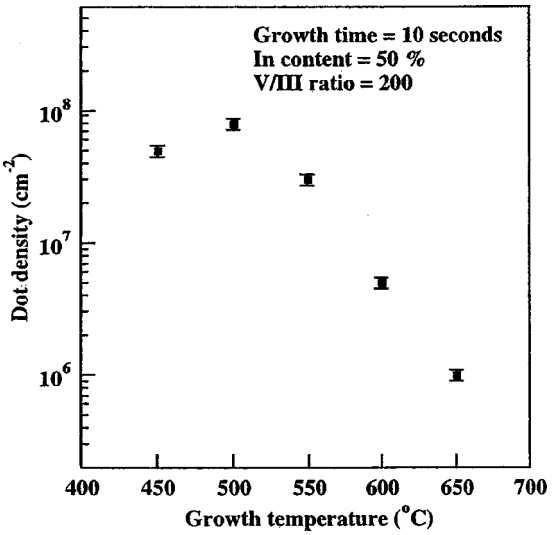

FIG. 2. Logarithmic plot of island density as a function of growth temperature at a fixed V/III ratio, In content, and growth time.

growth time, and In composition. Atomic force microscope (AFM) measurement was carried out to characterize the island size and density.

For the fabrication of laser diode an initial 10 nm thick undoped GaAs nucleation layer was deposited on Si substrate at 400 °C. Further, the growth temperature was raised to 750 °C and a 1 μm thick n^+-GaAs buffer layer (Se-doped, 2×10^{18} cm^{-3}) was grown. Over the buffer layer a 1.0 μm thick n-$Al_{0.7}Ga_{0.3}As$ lower cladding layer, a 70 nm thick undoped $Al_{0.3}Ga_{0.7}As$ lowering confining layer, an active layer containing $In_xGa_{1-x}As$ (In=0.1, 0.2, 0.3, 0.4) QD, a 70 nm thick undoped $Al_{0.3}Ga_{0.7}As$ upper confining layer, a 1.0 μm thick p-$Al_{0.7}Ga_{0.3}As$ upper cladding layer, and an 80 nm thick p^+-GaAs (Zn-doped, 1×10^{18} cm^{-3}) contact layer were grown in order to realize the laser diode structure as shown in Fig. 1. After the growth, the laser devices were processed as follows: a 0.1 μm thick SiO_2 insulating layer was deposited on the p^+-GaAs contact layer and 10 μm wide stripe contact windows were opened with a 300 μm pitch along the $\langle 110\rangle$ direction by chemical etching ($HF:NH_4F:CH_3COOH=1:20:7$) of SiO_2. Then Ti/Au (50/150 nm) contacts were deposited by electron beam evaporation on the p^+-GaAs layer. After thinning the n^+-Si substrate to a thickness of 100 μm, AuSb/Au (50/150 nm) was deposited on the Si substrate in order to form the n-side electrode.

Injected current versus output current (I–L) characteristics and emission spectrum analysis were carried out to observe the lasing property of the laser diode. Automatic power controlled (APC) lifetime measurement has been performed in order to know the degradation mechanism of laser diodes.

III. RESULTS AND DISCUSSION

The formation of $In_xGa_{1-x}As$ islands/dots on GaAs/Si was found to depend on the different growth conditions. After the growth of $In_xGa_{1-x}As$ islands/dots on GaAs/Si, the surface morphology was observed with AFM. Figure 2 shows the logarithmic plot of island density as a function of growth temperature at fixed values of V/III ratio, In content, and growth time. It is observed that the dependence is not linear over the entire temperature range, though a decrease in island density with increasing temperature is revealed. This indicates that more than one kinetic process is competing to control the formation of the $In_xGa_{1-x}As$ island on GaAs/Si. The decrease in island density with increasing substrate temperature may be qualitatively reconciled as being a consequence of the thermally enhanced surface migration of In.

The dependence of island density with respect to the variation of In content at fixed values of growth temperature, time, and V/III ratio is shown in Fig. 3. The figure reveals that there is an increase in island density with the increase in In content, but the size nonuniformity is severe in the case of higher percentage of In. In principle, In content has an important role in the formation of islands since the formation of islands/dots by SK growth mode is a strain-induced effect in a lattice-mismatch system. The bulk lattice mismatch be-

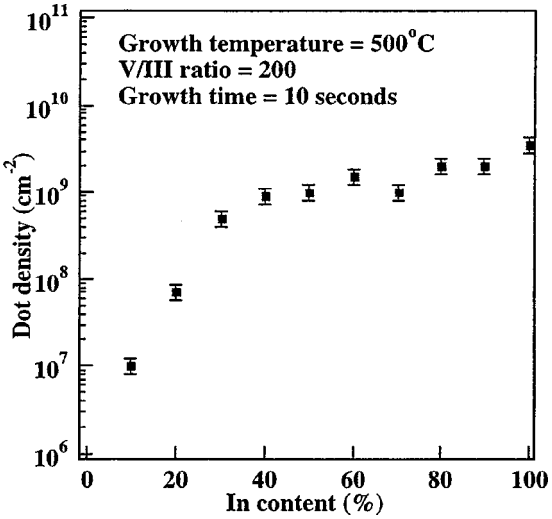

FIG. 3. Variation of dot density of InGaAs on Si substrate with respect to In content.

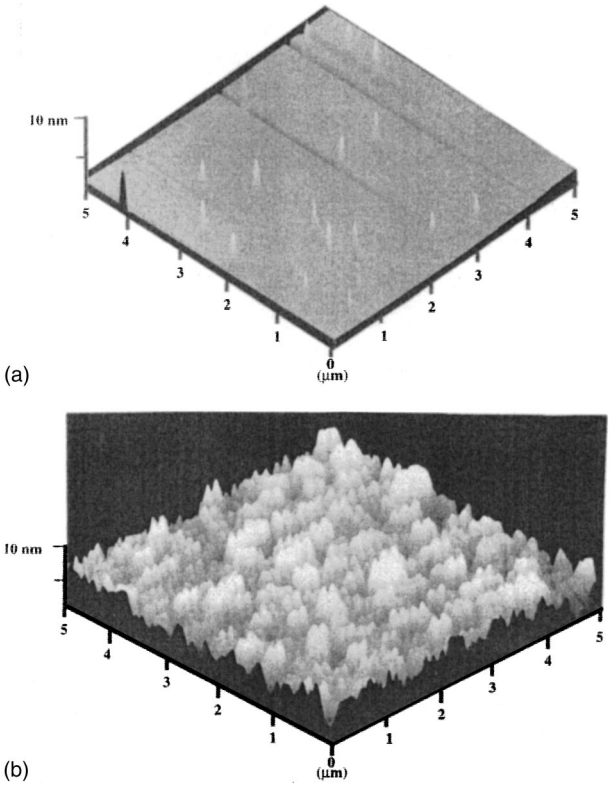

FIG. 4. AFM images of a typical InGaAs dot on Si with In content (a) 20% and (b) 100%.

tween InAs and GaAs is ~7% and also there is a 4% lattice mismatch between GaAs and Si. As a result, the strain distribution in the system of $In_xGa_{1-x}As/GaAs/Si$ is more or less complicated. The AFM study reveals that two types of growth mode are operative depending upon the In content: (1) layer by layer growth mode below $x=0.2$ and (2) three-dimensional island growth mode above $x=0.3$.

Further, lower content of In, for instance in the $In_{0.2}Ga_{0.8}As$ system, results in discrete dots with an average interdot distance of 2 μm [Fig. 4(a)], while for InAs [Fig. 4(b)] the dots appear locally connected in agglomerations. The above observation once again implies that the onset of dot formation is governed by strain energy.[22,23]

The growth of islands also depends upon the V/III ratio, which controls the availability of the constituents for the growth. The As, Ga, and In reach the growing islands via intraplanar surface migration. Even for sufficient intraplanar migration of Ga and In, the ability of both is an important parameter to be considered. Figure 5 shows the variation of dot density of InGaAs on Si with respect to the group V/III ratio. It is found that as the V/III ratio decreases, the dot density increases. But, too much reduction in the V/III ratio results in overlapping of the dots. Figure 6 shows the AFM images of InGaAs QD on Si for two different V/III ratios [(a) 68 and (b) 50]. In the case of Fig. 6(a) (V/III ratio of 68) the dots are discrete with a dot density of $\sim 10^9/cm^2$ and the interdot mean distance is 400 nm, whereas in Fig. 6(b) (V/III ratio of 50), the dots are interlinked and in some places overlapped with a density of $\sim 10^{11}/cm^2$. The effective diameter of these dots varies from 20 to 30 nm. Even though the dot

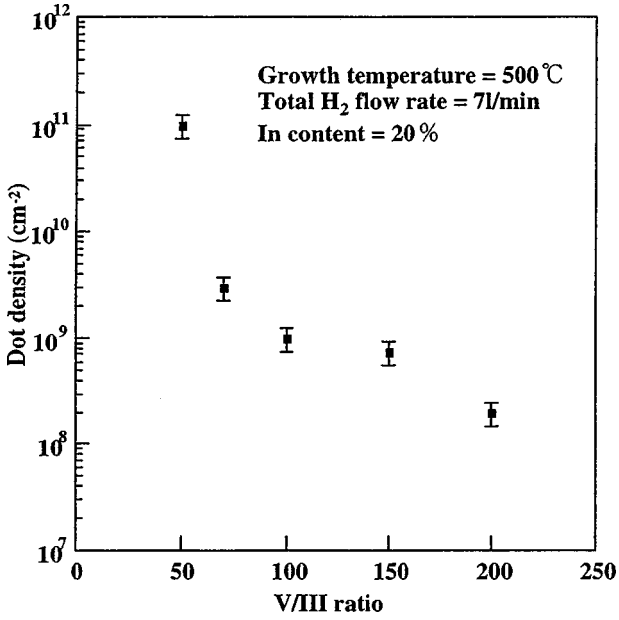

FIG. 5. Variation of dot density of InGaAs on Si with respect to group V/III ratio.

density is higher in the second case, the dots are shapeless and therefore can hardly be considered as quantum dots. From the crystal growth point of view, the growth rate is controlled by the group-III flux whose incorporation is unity and the growth kinetics is controlled by the adsorption rate of group-V elements. In the case of higher V/III ratio, the As incorporation rate becomes slow, since group-III migration inhibits the subsequent arrival of additional group-III atoms due to the allotment of the sites for As incorporation and which results in discrete QD growth. On the other hand, in

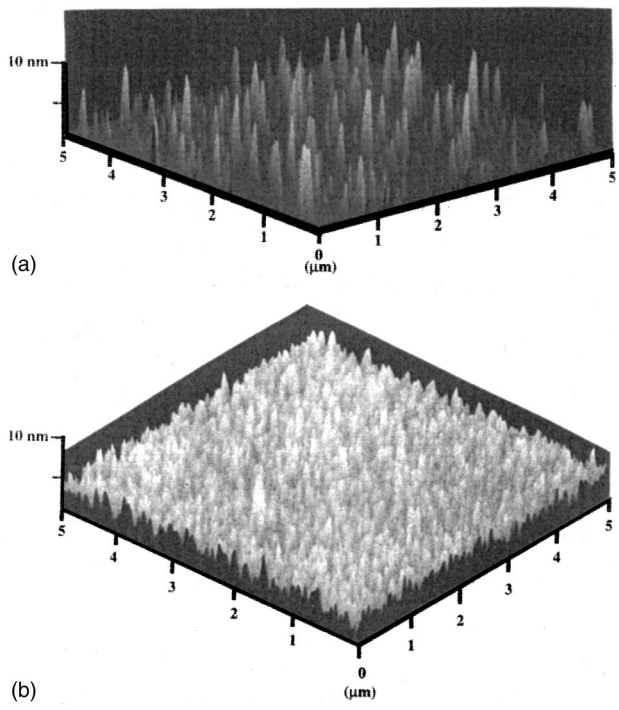

FIG. 6. AFM images of a typical $In_{0.2}Ga_{0.8}As$ dot on Si with V/III ratio (a) 68 and (b) 50.

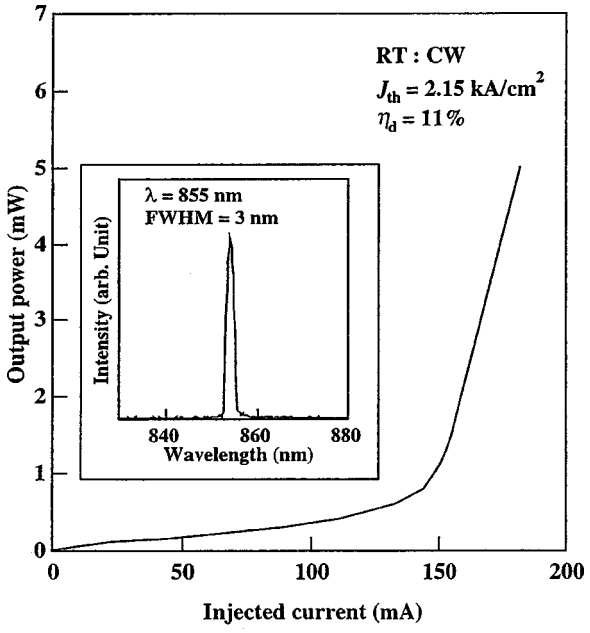

FIG. 7. $I-L$ characteristics and emission spectrum of the $In_{0.1}Ga_{0.9}As$ QW laser on Si substrate.

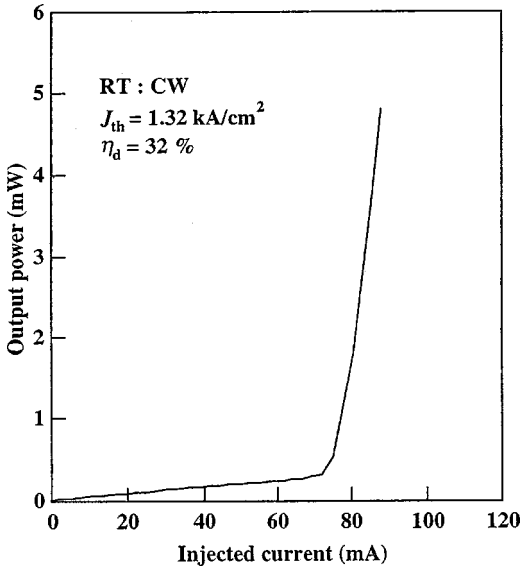

FIG. 8. $I-L$ characteristics of the $In_{0.1}Ga_{0.9}As$ QD-like laser on Si substrate.

the case of extremely lower V/III ratio, the unavailability of As leads to the formation of Ga or In-rich droplets and the extension of their size makes then join together due to the higher wetting capability. So, the droplets are not discrete in nature and it is believed that they are not useful for the further application of QD device fabrication. The observation of very high dot density may also not be real due to the interlinked nature of the dots.

Lasing characteristics measurements were carried out for the lasers with a QD-like active region containing InGaAs (In=10%, 20%, 30%, 40%). It is notable that the formation of dots was not realized with the In content 10%. Therefore the laser fabricated with the In content of 10% is considered as a quantum well (QW) laser. Figure 7 shows the typical injection current versus light output ($I-L$) characteristics of an $In_{0.1}Ga_{0.9}As$ QW laser measured at RT under cw condition. This laser shows a threshold current density of 2.15 kA/cm^2 with an external differential quantum efficiency of 11%. The emission spectrum is also shown in the inset of Fig. 7. Ground state emission is observed at 855 nm.

$I-L$ characteristics of the laser with an $In_{0.2}Ga_{0.8}As$ QD-like active region measured at RT, under cw conditions is shown in Fig. 8. The measurement reveals that the threshold current density (J_{th}) is 1.32 kA/cm^2 with an external differential quantum efficiently (η_d) of 32%. This threshold current density is comparatively lower than the GaAs-based quantum well laser on Si.[21] An ideally low-dimensional QD as the gain medium is expected to result in an ultralow threshold current by modifying the density of states function and differential gain. But, in practice, the size fluctuation of the dots severely affects the threshold current density. Further, the dots are accompanied by a two-dimensional layer called a wetting layer, which is acting as a relaxing medium for the diffusively injected carriers through the barrier layer. Some carriers recombine radiatively or nonradiatively both outside (wetting layer) and inside the dots. The injected carriers into the ground state emit photons to the lasing mode primarily due to the stimulated emission process, whereas the carrier injection into the higher energy levels have a higher probability of nonradiative recombination due to an increased number of recombination paths. The properly sized QDs result in lower defect density and enhance the carrier injection from the ground state. If the presence of nonradiative recombination centers are eliminated from the dots, then the threshold current density will be substantially reduced.

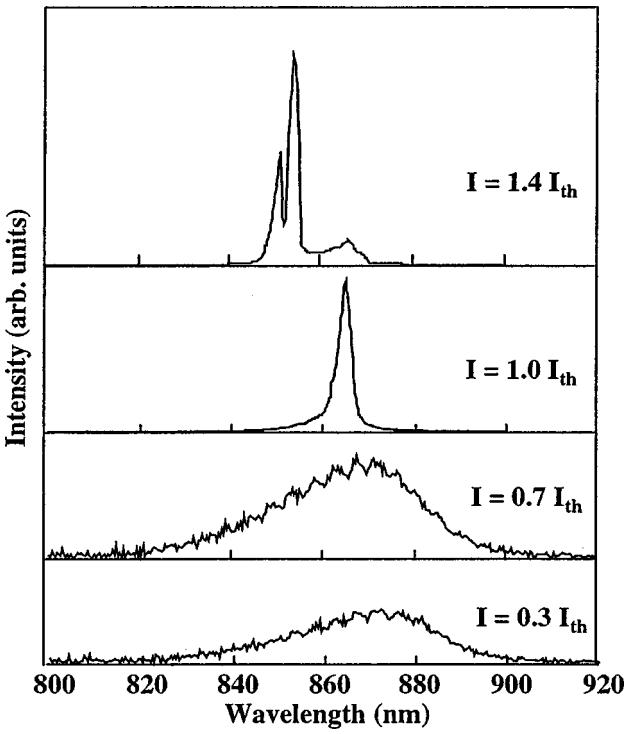

FIG. 9. Emission spectra of the $In_{0.2}Ga_{0.8}As$ quantum dot-like laser on a Si substrate at different currents.

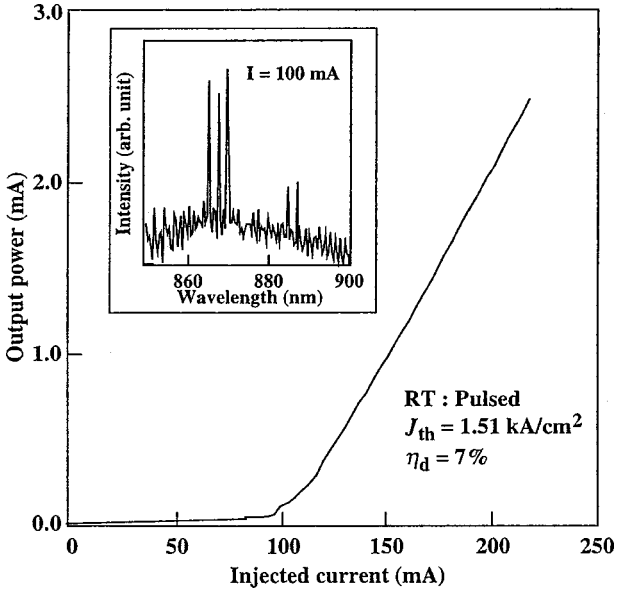

FIG. 10. $I-L$ characteristics and emission spectrum of the $In_{0.3}Ga_{0.7}As$ QD-like laser on Si.

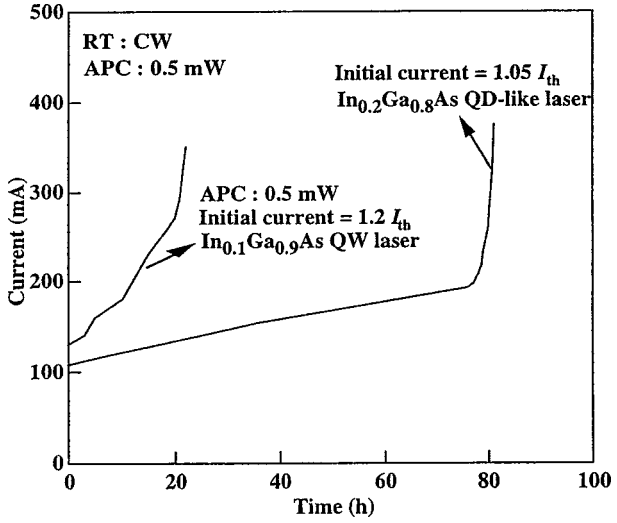

FIG. 12. Aging result of the $In_{0.1}Ga_{0.9}As$ QW and $In_{0.2}Ga_{0.8}As$ QD-like laser on a Si substrate at room temperature under the automatic power control condition.

The observation of reduced threshold current density for the QD-like laser diode is in good agreement with the above-said principle.

Figure 9 shows the applied current dependent emission spectra of a $In_{0.2}Ga_{0.8}As$ QD-like laser on Si. Lasing starts at a threshold current of 1.4 I_{th} at a wavelength of 854 nm. Below the threshold current, the emission peak is observed at the wavelength of 872 nm. As the injection current increases, emission peak shifts from the longer wavelength region to the shorter wavelength region. However, the initially observed peak at the longer wavelength region appears with extremely low intensity. This is attributed to the reduction of the ground state gain of the dots as a result of thermally activated carrier loss and the increased band-filling in the first excited state as the ground state gain becomes saturated.[24]

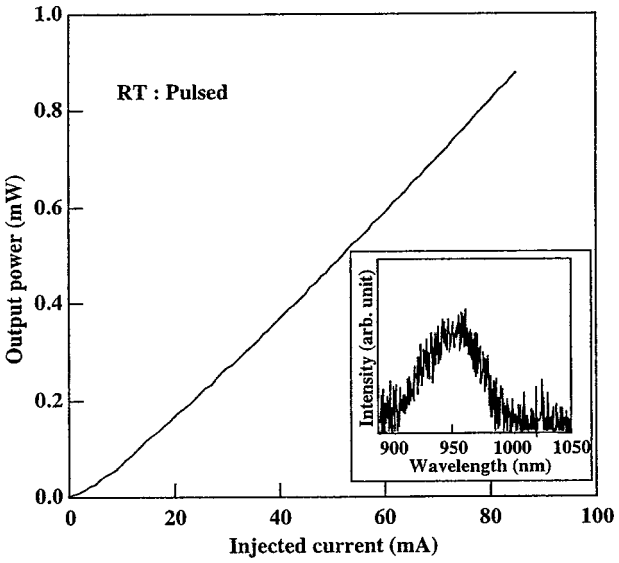

FIG. 11. $I-L$ characteristics and emission spectrum of the $In_{0.4}Ga_{0.6}As$ QD-like laser on Si.

$I-L$ characteristics with emission spectrum for the $In_{0.3}Ga_{0.7}As$ and $In_{0.4}Ga_{0.6}As$ QD-like laser on Si under a RT pulsed condition are shown in Figs. 10 and 11, respectively. The laser with an $In_{0.3}Ga_{0.7}As$ QD-like active region shows a J_{th} of 1.51 kA/cm^2 with an η_d of 7% (Fig. 10), while the laser with an $In_{0.4}Ga_{0.6}As$ active region shows no lasing (Fig. 11) at the RT pulsed mode. The failure of lasing in these lasers is due to the inferior dot quality. The increase in In content in the active region increases the bending of threading dislocations caused by increased strain.[25–27] The threading dislocations may also influence the carriers occupying higher energy levels and can cause more severe nonradiative recombination and modulation of the losses by constructive interference with the reflection of a transverse leaky mode propagating in the transparent substrate, thus decreasing the radiative efficiency of the In rich QD-like dot lasers. The observed lasing emission with broad and splited peaks shown in Fig. 10 for an $In_{0.3}Ga_{0.7}As$ QD-like active region is in agreement with the above discussion.

The aging results under an APC condition for the $In_xGa_{1-x}As$ QD-like lasers on Si are shown in Fig. 12. The lasers were operated at the cw constant output power of 0.5 mW at a heat-sink temperature of 300 K. For the laser with an $In_{0.2}Ga_{0.8}As$ QD-like active region, first the operating current increased at a rate of ~1 mA/h for 78 h, after which a sudden increase was observed over the remaining lifetime of the device while the laser with an $In_{0.1}Ga_{0.9}As$ QW active region degraded within 20 h. The conventional GaAs-based laser on Si shows a rapid degradation, due to the high order of dislocation density in the active region.[28] The ⟨100⟩ dark line defect (DLD) results from the formation of a complicated dislocation network due to the climbing motion from a dislocation that is grown in the buffer layer during the crystal growth due to lattice mismatch.

The gradual degradation in the earlier stage of the aging test of the $In_{0.2}Ga_{0.8}As$ QD-like laser on Si indicates that the

insertion of a dot-like active region suppresses the formation of DLD or dark spot defects (DSDs) in the dot regions. However, the failure of stability for a longer duration is attributed to the elongation of the dislocation network towards the dot region from the nondot region or gradual condensation of point defects in the dots or melting or destruction of the light emitting part at the facet due to the joule heating.

IV. CONCLUSION

The growth conditions of QD-like dots on Si substrates by the SK growth mode have been optimized using MOCVD. QD-like structures were optimized by considering the growth temperature, V/III ratio, and In content. Optimized QD-like structures were further used to fabricate laser diodes on Si substrates. The $In_{0.2}Ga_{0.8}As$ QD-like active region showed room temperature cw light emission with a lowest threshold current density of 1.32 kA/cm^2 in our experiment. The shift of the lasing wavelength towards the shorter region in the case of an $In_{0.2}Ga_{0.8}As$ QD-like laser was explained as band filling effect. The laser with an $In_{0.3}Ga_{0.7}As$ QD-like active region showed a threshold current density of 1.51 kA/cm^2 under RT pulsed condition. Lasing emission of the same laser was broad and consisted of splited peaks due to the nonuniform distribution of the electronic states of the dots. The aging test of this laser revealed that QD-like lasers are more reliable than the QW lasers realized by the same structure on Si. It is believed that proper optimization of size and density of QD can provide the reliable lasers on Si substrate.

[1] H. K. Choi, J. P. Mattia, G. W. Turner, and B. Y. Tsaur, IEEE Electron Device Lett. **9**, 512 (1988).
[2] H. Shichijo, R. Matyi, A. H. Taddiken, and Y. C. Kao, IEEE Trans. Electron Devices **37**, 548 (1990).
[3] T. Egawa, T. Jimbo, and M. Umeno, IEEE Photonics Technol. Lett. **4**, 612 (1992).
[4] T. Egawa, T. Jimbo, and M. Umeno, IEICE Trans. Electron. **E76-C**, 106 (1993).
[5] G. N. Nasserbakht, J. W. Adkisson, B. A. Wooly, J. S. Harris, and T. I. Kamis, IEEE J. Solid-State Circuits **28**, 622 (1993).
[6] I. Hayashi, Jpn. J. Appl. Phys., Part 1 **32**, 266 (1993).
[7] H. B. Kroemer, Mater. Res. Soc. Symp. Proc. **67**, 3 (1986).
[8] R. L. Hartman and A. R. Hartman, Appl. Phys. Lett. **23**, 147 (1973).
[9] T. Kamejima, K. Ishida, and J. Matsui, Jpn. J. Appl. Phys., Part 1 **16**, 233 (1977).
[10] A. R. Goodwin, P. A. Kirkby, I. G. Davies, and R. S. Baulcomb, Appl. Phys. Lett. **34**, 647 (1979).
[11] T. Egawa, A. Ogawa, T. Jimbo, and M. Umeno, Jpn. J. Appl. Phys., Part 1 **37**, 1552 (1998).
[12] M. Akiyama, Y. Kawarada, and K. Kaminishi, Jpn. J. Appl. Phys., Part 2 **23**, L843 (1984).
[13] W. T. Masselink, T. Henderson, J. Klem, R. Fischer, P. Pearah, H. Morcok, M. Hafich, P. D. Wang, and G. Y. Robinson, Appl. Phys. Lett. **45**, 1309 (1984).
[14] R. Fischer, D. Neuman, H. Zabel, H. Morcok, C. Choi, and N. Otsuka, Appl. Phys. Lett. **48**, 1223 (1986).
[15] G. M. Metze, H. K. Choi, and B. Y. Tsaur, Appl. Phys. Lett. **45**, 1107 (1984).
[16] L. Goldstein, F. Glas, J. Y. Marzin, M. N. Charase, and G. Leroux, Appl. Phys. Lett. **47**, 1099 (1985).
[17] P. R. Berger, K. Chang, P. Bhattacharya, J. Singh, and K. K. Bajaj, Appl. Phys. Lett. **53**, 684 (1988).
[18] K. K. Linder, J. Philips, O. Qasaimeh, X. F. Liu, S. Krishna, P. Bhattacharya, and J. C. Jiang, Appl. Phys. Lett. **74**, 1355 (1999).
[19] E. P. O'Reilly, Semicond. Sci. Technol. **4**, 121 (1989).
[20] H. Shoji, K. Mukai, N. Ohtsuka, M. Sugawara, T. Uchida, and H. Ishikawa, IEEE Photonics Technol. Lett. **7**, 1385 (1995).
[21] T. Egawa, Y. Hasegawa, T. Jimbo, and M. Umeno, Jpn. J. Appl. Phys., Part 1 **31**, 791 (1992).
[22] V. A. Shchukin, N. N. Ledentsov, P. S. Kop'ev, and D. Bimberg, Phys. Rev. Lett. **74**, 4043 (1995).
[23] V. A. Shchukin, N. N. Ledentsov, M. Grundmann, P. S. Kop'ev, D. Bimberg, and V. M. Ustinov, Surf. Sci. **352-354**, 117 (1996).
[24] D. G. Deppe, D. L. Huffaker, S. Csutak, Z. Zou, G. Park, and O. B. Shchekin, IEEE J. Quantum Electron. **35**, 1238 (1999).
[25] J. J. Coleman and K. J. Beernink, J. Appl. Phys. **75**, 1879 (1994).
[26] E. Yablonovitch and E. O. Kane, J. Lightwave Technol. **4**, 504 (1986).
[27] I. Suemune, IEEE J. Quantum Electron. **27**, 1149 (1991).
[28] Y. Hasegawa, T. Egawa, T. Jimbo, and M. Umeno, Jpn. J. Appl. Phys., Part 1 **34**, 2994 (1995).